


Phytoconstituents from *Adenantha pavonina* L. as antioxidants and inhibitors of inducible TNF- α production in BV2 cells

Shaymaa M. Mohamed, Emad H. M. Hassanein, Samir A. Ross & Nesma M. Mohamed


To cite this article: Shaymaa M. Mohamed, Emad H. M. Hassanein, Samir A. Ross & Nesma M. Mohamed (2022): Phytoconstituents from *Adenantha pavonina* L. as antioxidants and inhibitors of inducible TNF- α production in BV2 cells, Natural Product Research, DOI: [10.1080/14786419.2022.2027938](https://doi.org/10.1080/14786419.2022.2027938)



To link to this article: <https://doi.org/10.1080/14786419.2022.2027938>

 View supplementary material 

 Published online: 25 Jan 2022.

 Submit your article to this journal 



 Article views: 52

 View related articles 

 View Crossmark data 



Phytoconstituents from *Adenantha pavonina* L. as antioxidants and inhibitors of inducible TNF- α production in BV2 cells

Shaymaa M. Mohamed^a , Emad H. M. Hassanein^b , Samir A. Ross^{c,d} and Nesma M. Mohamed^a

^aDepartment of Pharmacognosy, Faculty of Pharmacy, Assiut University, Assiut, Egypt; ^bDepartment of Pharmacology and Toxicology, Faculty of Pharmacy, Al-Azhar University, Assiut, Egypt; ^cNational Center for Natural Products Research, Research Institute of Pharmaceutical Sciences, School of Pharmacy, The University of Mississippi, Oxford, MS, USA; ^dDepartment of Biomolecular Sciences, Division of Pharmacognosy, School of Pharmacy, University of Mississippi, Oxford, MS, USA

ABSTRACT

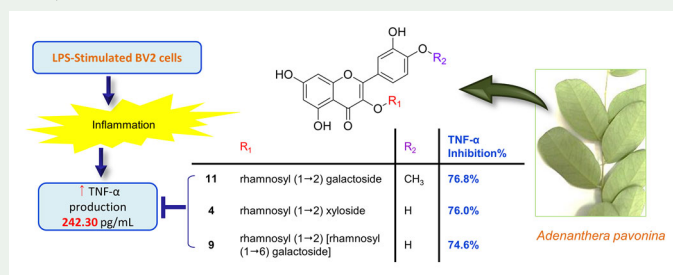
Adenantha pavonina L. has been used traditionally to relieve inflammation. This study aimed to expand the phytochemical knowledge of *A. pavonina* and evaluate its constituents for their antioxidant and anti-inflammatory potentials as tumor necrosis factor alpha (TNF- α) inhibitors. The antioxidant activity was evaluated using the DPPH radical scavenging assay, and the inhibition of TNF- α was assessed through ELISA and qRT-PCR techniques. Interestingly, five previously undescribed metabolites, including a pentadienoic acid derivative, a triterpenoid glycoside, and three tamarixetin glycosides, were identified alongside seven known compounds. Most compounds evaluated had higher DPPH radical scavenging capabilities than the standard, trolox. Tamarixetin 3-O-(α -L-rhamnopyranosyl)-(1 \rightarrow 2)- β -D-galactopyranoside (**11**), a previously undescribed compound, was the most effective at suppressing TNF- α protein and m-RNA levels. Other flavonoid glycosides, quercetin 3-O-(α -L-rhamnopyranosyl)-(1 \rightarrow 2)- β -D-xylopyranoside (**4**), isovitixin (**5**), and quercetin-3-O-[α -L-rhamnopyranosyl-(1 \rightarrow 2)]-[α -L-rhamnopyranosyl-(1 \rightarrow 6)]- β -D-galactopyranoside (**9**), also significantly lowered TNF- α production.

ARTICLE HISTORY


Received 18 November 2021
Accepted 2 January 2022

KEYWORDS

Adenantha pavonina;
Fabaceae; flavonol
glycosides; antioxidant;
anti-inflammatory; TNF- α
inhibition



CONTACT Samir Anis Ross  sross@olemiss.edu

 Supplemental data for this article can be accessed online at <https://doi.org/10.1080/14786419.2022.2027938>.

© 2022 Informa UK Limited, trading as Taylor & Francis Group

1. Introduction

Inflammation is a serious condition that occurs in conjunction with several diseases afflicting humans (Wang et al. 2021). Chronic inflammation causes damaging cellular and vascular changes, oxidative stress, and over-expression of various pro-inflammatory cytokines including TNF- α and Interleukins (ILs) (Medzhitov 2010). A vast array of pathological conditions are also associated with activation of TNF- α (Giollo et al. 2021). Thus, TNF- α inhibitors could avoid the serious untoward effects of the conventional anti-inflammatory NSAIDs and glucocorticoids (Wongrakpanich et al. 2018).

Adenantha pavonina L. (Fabaceae) is a wild ethno-medicinal tree endemic to India, South-East China, and Malaysia. Earlier phytochemical research on the plant revealed a variety of bioactive phytochemicals, including sterols, fatty acids, pavonin lactone, flavonoids, and their glycosides (Gennaro et al. 1972; Ali et al. 2005; Mohammed et al. 2014). Several traditional applications of the plant have been reported in diarrhea, hemorrhagic conditions, rheumatism, lung ailments, and gout, reflecting its astringent and anti-inflammatory potentials (Khare 2007). Olajide et al. have demonstrated the analgesic and anti-inflammatory effects of its seed extract (Olajide et al. 2004). A decoction containing *A. pavonina* has displayed a cytotoxic effect against human laryngeal carcinoma (Lindamulage and Soysa 2016). These traditional uses and medicinal importance fueled our interest in exploring the incompletely studied phytochemical profile of the aerial parts.

Flavonoid glycosides were found to be the major components in this phytochemical investigation of *A. pavonina*. Several studies have proved the antioxidant and anti-inflammatory activities of flavonoid derivatives through various mechanisms (Okawa et al. 2001; Choy et al. 2019; Habib et al. 2020; Owor et al. 2020). Based on the reported anti-inflammatory activities of *A. pavonina* and structurally related compounds to the plant's isolated constituents, selected isolates were assessed for their antioxidant and anti-inflammatory capacities to attenuate the LPS-induced inflammatory response in BV2 cells.

2. Results and discussion

2.1. Phytochemical investigation

The chromatographic analysis resulted in isolation and identification of five previously undescribed compounds (**1**, **3**, **8**, **11**, and **12**) (Chart 1). Compound **1**, a white amorphous powder, had a molecular formula of $C_{20}H_{28}O_{10}$ with seven degrees of unsaturation based on the detected molecular ion peak at m/z 427.1608 $[M-H]^-$ (calcd 427.1604) in High Resolution Electrospray Ionization Mass Spectrometry (HRESIMS) spectrum (negative mode). The 1H NMR spectrum displayed two *trans*-olefinic protons at δ_H 7.90 and 6.35 (each *d*, $J = 15.9$ Hz), a methyl singlet at δ_H 2.03, and an olefinic proton H-2 at δ_H 5.75. These signals are characteristic features for the substructure (3-methyl-2*E*,4*E*-pentadienoic acid) (Sasaki et al. 1991). HMBC correlations (Figure S6, [supplementary material](#)) supported the position of methyl group and other functions in this substructure. For example, H-2 showed strong HMBC correlations with two carbons that resonating at δ_C 131.0 and 20.6. The configuration of the two double bonds was assigned

as *trans* based on the coupling constants of H-4 and H-5 along with NOESY correlations between H-5 and 3-Me group. In addition, a substituted cyclohexyl moiety, attached to C-5, was deduced from the detailed analysis of NMR spectral data (Table S1, Figures S1–S7, [supplementary material](#)). The ^1H NMR spectrum exhibited two singlets corresponding to additional two methyl substituents on the cyclohexyl moiety resonating at δ_{H} 1.24 and 0.95. The former methyl group showed significant HMBC correlations to carbons at δ_{C} 81.0, 87.9, and 41.3 (C-1', 2', and 3') confirming its angular location at C-2'. The other methyl group showed HMBC correlations with a quaternary carbon at δ_{C} 51.8 (C-6') and a carboxy group at δ_{C} 178.2 (6'-COOH) suggesting the presence of methyl and carboxylic functions attached to C-6'. An oxygenated methine (H-4) was detected at δ_{H} 3.63 and located at C-4' flanked by the two methylenes (C-3' and C-5') of the cyclohexyl ring based on ^1H - ^1H COSY correlations. The β -configuration of the hydroxyl function at C-4' was judged from the observed multiplicities of H-4 (Rodríguez-Deleón et al. 2019). The DEPTQ-135 spectrum confirmed the deduced structural fragments and showed the presence of two additional carbonyl groups at δ_{C} 173.9 and 177.3 together with a methyl group at δ_{C} 17.3 (*d*, 7.15), a methylene at δ_{C} 38.9, and a methine at δ_{C} 36.1 suggesting the presence of (2-methylsuccinyl) fragment. The HMBC and ^1H - ^1H COSY correlations ([Figure S4–6](#), [supplementary material](#)) clearly confirmed the succinyl structural assignment. The relative configurations at C-2'', C-2', and C-6' were postulated through the NOESY experiment which showed no cross peaks between H-4' and any of the methyl signals 2'-Me, 6'-Me or 2''-Me. The configuration at C-1' was not identified because the small amount of **1** limited further analysis. Accordingly, the structure of **1** was identified as 5-[1',4'-dihydroxy-2',6'-dimethyl-6'-carboxy-2'-(2''-methyl-succinyloxy) cyclohexyl]-3-methyl-2*E*,4*E*-pentadienoic acid which is a previously undescribed natural metabolite. This class is reported herein for the first time from the genus.

Compound **3**, a yellow-brown powder, was assigned the molecular formula of $\text{C}_{27}\text{H}_{30}\text{O}_{15}$ based on HRESIMS spectra which displayed molecular ion peaks at m/z 593.1504 $[\text{M} - \text{H}]^-$ (calcd 593.1506) in the negative mode and m/z 617.1482 $[\text{M} + \text{Na}]^+$ (calcd 617.1482) in the positive mode. The ^1H NMR spectral data (Table S2, [supplementary material](#)), showed a characteristic flavonol glycoside pattern with an ABX spin system assigned to ring B protons and two meta-coupled signals of ring A protons. Additionally, a sharp singlet at δ_{H} 3.86 was observed corresponding to a methoxy group which showed HMBC correlation to C-4' of the aglycone indicating a tamarixetin (4'-methoxy quercetin) aglycone. Regarding the saccharide moiety, diagnostic signals for α -L-rhamnopyranosyl unit were detected at δ_{H} 5.08 (*br s*, H-1''') and 0.872, (*d*, 6.0, H-6''')/ δ_{C} 101.2 (C-1''') and 17.9 (C-6'''). Additional pentose sugar was deduced from its anomeric peaks, resonating at δ_{H} 5.53 (*d*, $J = 7.2$ Hz, H-1'') and δ_{C} 100.1 (C-1'') together with the remaining signals that are consistent with those of β -D-xylopyranosyl moiety (Table S2) (Agrawal 1989; Phechrmeekha et al. 2012). Complete assignment of the two sugars was established by HSQC spectrum. C-1''' of the rhamnopyranosyl moiety showed HMBC correlation with H-2'' (3.55) of the xylopyranoside and H-1'' exhibited 3J -correlation with C-3 (133.7) confirmed the attachment of α -L-rhamnopyranosyl-(1 \rightarrow 2)- β -D-xylopyranosyl moiety at C-3 ([Figure S12](#), [supplementary material](#)). Thus, **3** was elucidated as tamarixetin-3-O- α -L-

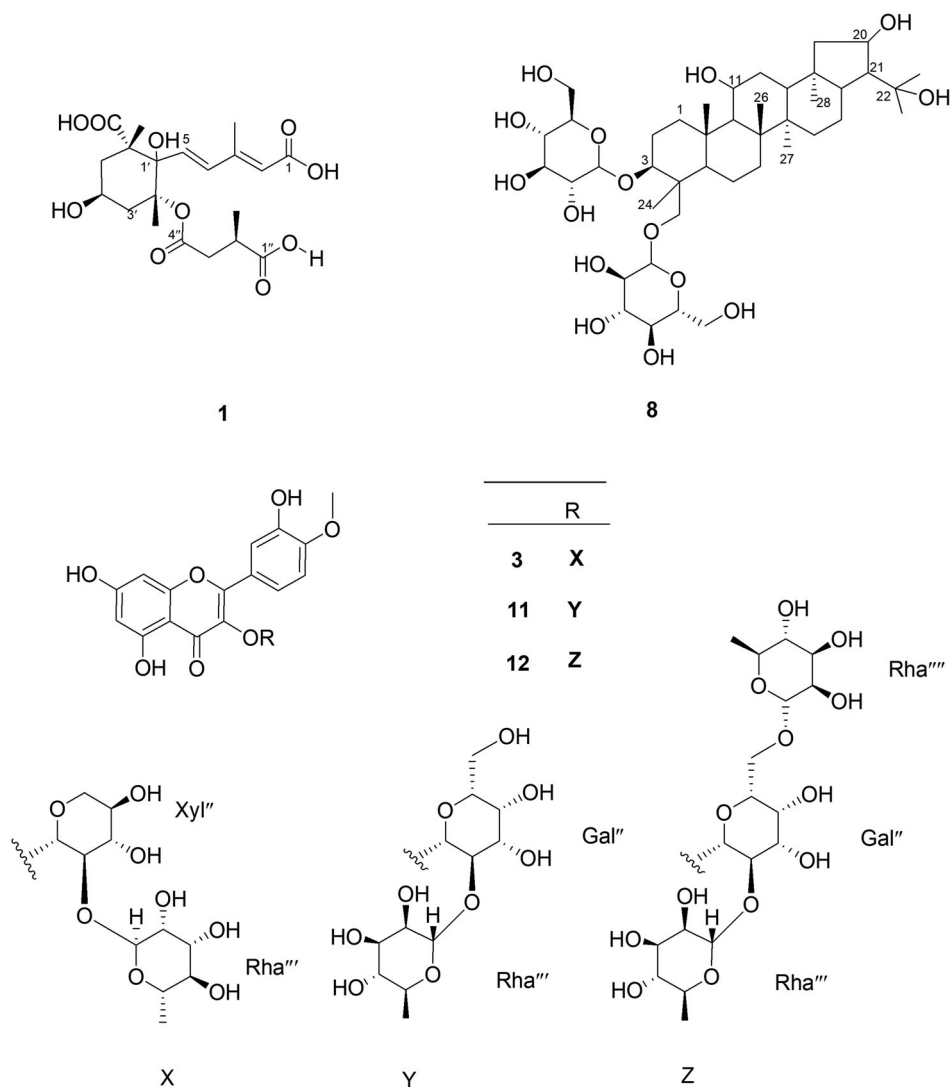


Chart 1. Structures of previously undescribed compounds.

-rhamnopyranosyl-(1→2)- β -D-xylopyranoside. Notably, this is the first report for this compound from nature.

The NMR spectral data (Table S2, [supplementary material](#)) indicated that compounds **11** and **12** have the same aglycone (tamarixetin) as **3** but with different saccharide residues attached to C-3. Compound **11** was given the molecular formula $C_{28}H_{32}O_{16}$ based on the positive HRESIMS spectrum which displayed a molecular ion peak $[M + Na]^+$ at m/z 647.1507 (calcd 647.1588 $C_{28}H_{32}O_{16}Na^+$). The 1H NMR spectrum showed two anomeric protons of a disaccharide, including a doublet at δ_H 5.63 ($J = 7.6$ Hz) for a 3- O - β -D-galactopyranoside moiety, completely characterized through HSQC and 1H - 1H COSY, and a broad singlet at δ_H 5.02 together with a doublet at δ_H 0.75 ($J = 6.0$ Hz), assigned to the anomeric and the methyl group protons of α -L-rhamnopyranosyl unit. A long-range HMBC correlation was observed between C-3 (δ_C

133.4) and H-1'' at δ_{H} 5.63 confirming the site of glycosylation. The downfield shifting of C-2'' (δ_{C} 75.3) than the reported value (δ_{C} 73.2) (Shahat et al. 2001) suggested the placement of the α -L-rhamnosyl unit at this position. This was further confirmed by the long range HMBC correlations from H-2'' (δ_{H} 3.79) to C-1'' (δ_{C} 99.1) and C-1''' (δ_{C} 100.6), and from H-1''' (δ_{H} 5.02) to C-2'' (δ_{C} 75.3) (Figure S24, [supplementary material](#)). Thus, **11** was identified as tamarixetin 3-O-(α -L-rhamnopyranosyl)-(1 \rightarrow 2)- β -D-galactopyranoside, which is a new compound.

The molecular formula of **12** was determined to be $\text{C}_{34}\text{H}_{43}\text{O}_{20}$ according to the negative HRESIMS spectrum which displayed two molecular ion peaks at m/z 769.2227 $[\text{M} - \text{H}]^-$ (calcd 769.2191 $\text{C}_{34}\text{H}_{41}\text{O}_{20}^-$) and 805.1998 $[\text{M} + \text{Cl}]^-$ (calcd. 805.2036 $\text{C}_{34}\text{H}_{43}\text{O}_{20}\text{Cl}^-$). Inspection of its NMR spectral data (Table S2, [supplementary material](#)) revealed great similarity with that of **11** except for the presence of an additional α -L-rhamnopyranosyl moiety. The placement of the additional rhamnose moiety at C-6'' of β -D-galactopyranosyl moiety was clearly established from the downfield shifting of this carbon to δ_{C} 65.3 than its value at β -D-galactopyranoside analogues with free C-6'' position ($\approx \delta_{\text{C}}$ 60.5) (Adell et al. 1988; Yasukawa et al. 1990). This assumption was further confirmed by HMBC correlations from the H-1'''' (δ_{H} 4.38) to C-6'' (δ_{C} 65.3), C-3'''' (δ_{C} 70.6), and C-5'''' (δ_{C} 68.3), and from H-6'' (δ_{H} 3.26) to C-1'''' (δ_{C} 100.2) and C-5'' (δ_{C} 75.8). Therefore, **12** was assigned as tamarixetin -3-O-[α -L-rhamnopyranosyl (1 \rightarrow 2)]-[α -L-rhamnopyranosyl (1 \rightarrow 6)]- β -D-galactopyranoside which is firstly reported from nature.

Compound **8** was isolated as a white amorphous powder. It was assigned the molecular formula $\text{C}_{42}\text{H}_{72}\text{O}_{15}$ as determined by positive mode HRESIMS (m/z 861.4810 $[\text{M} + \text{FA} - \text{H}]^-$, calcd for $\text{C}_{43}\text{H}_{73}\text{O}_{17}^-$, 861.4847). The ^1H NMR and DEPTQ-135 spectral data (Table S3, [supplementary material](#)) revealed its triterpenoid glycosidic nature. Based on the molecular formula, the index of hydrogen deficiency is seven, two attributed to the observed sugar residues, suggesting a pentacyclic skeleton of the sapogenin. The ^1H NMR displayed seven singlets at δ_{H} 0.56, 0.80, 0.82, 0.90, 1.12, 1.13, and 1.14 attributed to seven tertiary methyl groups, a hydroxymethylene at δ_{H} 3.26 and 3.48, and three oxymethines at δ_{H} 3.40, 3.55, and 4.13 along with two anomeric protons at δ_{H} 4.10 and 4.23 suggested a hydroxylated hopane-type triterpene glycoside. Observation of a characteristic doublet of doublets at δ_{H} 3.40 for the oxymethine proton H 3 α with determined couplings (J 11.2 and 5.6) assigned to $^3J_{(\text{H}3\alpha\text{-H}2\beta)}$ and $^3J_{(\text{H}3\alpha\text{-H}2\alpha)}$, respectively, firmly confirm its α orientation and established the β -configuration of 3-hydroxyl group (Wilkins et al. 1989; Riaz et al. 2013). The HMBC spectrum (Figure S18, [supplementary material](#)) exhibited alternating cross peaks between Me-29 and Me-30 and from both of them to the quaternary oxygenated C-22 at δ_{C} 74.9 which aided the assignments of these two methyl groups and firmly confirmed their presence at C-22. The location of the hydroxyl group at C-20 was evidenced based on the observed HMBC correlations from H-20 to C-22, ^1H - ^1H COSY between H-19 and H-20 and HMBC correlation from H-28 to C-19 which was suggestive of the linkages from C-18 to C-20, and the absence of any methylene signals around δ_{C} 41 (assigned for H-19 in most analogous 22-hydroxyhopane triterpenes lacking oxygenation at C-20). Concerning the saccharide, two β -D-glucopyranosyl moieties were observed with typical chemical shifts which located at C-3 and C-23 of the aglycone based on HMBC

correlations from H-1' to C-3 and from H-1'' to C-23. The β -configurations of the sugars were deduced from their large coupling constants. The configurations at chiral carbons C-11, 20, and 21 were not determined due to amount shortage. Based on the spectral data analysis, **8** was identified as 3-*O*- β -D-glucopyranosyl-23-*O*- β -D-glucopyranosyl-3 β , 11, 20, 22, 23-pentahydroxy-hopane, which is a new compound.

Structures of other compounds (**2**, **4–7**, **9**, and **10**) were confirmed through comparison of their spectral data with those reported ones. These isolates were elucidated as methyl gallate (**2**) (Ma et al. 2005), quercetin 3-*O*-(α -L-rhamnopyranosyl-(1 \rightarrow 2)- β -D-xylopyranoside (**4**) (Phechrmeekha et al. 2012), isovitixin (**5**) (Peng et al. 2008), quercetin-3-*O*- α -L-rhamnopyranoside (**6**) (Aderogba et al. 2012a), quercetin 3-*O*-(2''-*O*- α -L-rhamnopyranosyl-6''-*trans-p*-coumaroyl)- β -D-glucopyranoside (**7**) (Xu et al. 2009), quercetin-3-*O*-[α -L-rhamnopyranosyl (1 \rightarrow 2)]-[α -L-rhamnopyranosyl (1 \rightarrow 6)]- β -D-galactopyranoside (**9**) (Yasukawa et al. 1989), and isoschaftoside (**10**) (Fernando et al. 2019).

The genus *Adenantha* has been reported to have flavonoid glycosides; however, no previous studies have reported pentadienoic acid derivatives or hopane-type triterpene glycosides.

2.2. Effect of some isolated compounds on BV2 microglial cells viability

All investigated isolates did not exhibit cytotoxic effects on BV2 cells as indicated by their high IC₅₀ values. Calculated IC₅₀ values of the tested compounds are shown in (Table S4, [supplementary material](#)). These data indicate that the tested isolates have no influence on cell viability; hence, concentration of 100 μ M was used in subsequent experiments.

2.3. Effect of some isolated compounds on LPS-induced TNF- α activation

Elevated concentrations of both TNF- α protein and m-RNA were successfully induced in BV2 cells through LPS exposure to serve as a positive control. TNF- α was chosen as it plays an important role in inflammations, and its dysregulation has been linked to many human diseases (Halaris et al. 2012). The effects of compounds (**3–7**, **9**, **11**, and **12**) on the production of TNF- α were assessed; however, compounds **1**, **2**, **8**, and **10** were excluded from biological evaluations because of insufficient yields. The highest suppression in TNF- α protein level was observed with **11**, which was comparable to the normal secreted amount (the negative control). Compounds **4**, **5**, and **9** also displayed significant overall reduction of TNF- α release (Table S5, [supplementary material](#)). To determine whether the tested compounds inhibited TNF- α production at the transcriptional level or had post-transcriptional effects, the qRT-PCR analysis, a parallel experiment, was done. After 6 h, these compounds significantly reduced TNF- α mRNA expression, implying that they inhibited the gene expression of the tested cytokine (Table S5, [supplementary material](#)).

We found that quercetin derivatives **4**, **9**, and **11** reduce the pro-inflammatory mediator TNF- α secretion and downregulate the regulatory genes in LPS-stimulated BV2 microglia cells. These findings support a previous study in which quercetin has been shown to significantly reduce TNF- α production and gene expression in a dose-

dependent manner, indicating its ability to regulate the immune response and potential anti-inflammatory properties (Nair et al. 2006).

2.4. Antioxidant activities

All tested compounds, except **5**, effectively scavenged the DPPH radicals with IC_{50} values less than that of the positive control, trolox (IC_{50} 47.85 $\mu\text{g/mL}$). Compounds **6** and **7** were the most potent antioxidants with IC_{50} values of 18.24 and 16.42 $\mu\text{g/mL}$, respectively. The results are shown in (Table S6, [supplementary material](#)). These findings were consistent with previous structure activity studies that have linked antioxidant activity to the presence of 2, 3-unsaturation, 3', 4' catechol moiety, 3-OH group, and 4-keto functional group (Aderogba et al. 2012b). Accordingly, the lack of a catechol group in compound **5** (isovitexin) resulted in its inactivity, whereas co-existence of all required structural aspects was behind the observed antioxidant activities of other quercetin glycosides investigated.

3. Experimental

3.1. General phytochemical experimental procedures

Specific rotations were measured using a Rudolph Research AutoPol IV polarimeter (Rudolph Research Analytical, Hackettstown, NJ, USA) at room temperature. The NMR spectra were recorded on Bruker Avance DRX spectrometer at 400 MHz and 500 MHz (Bruker Scientific Instruments, MA, USA) using TMS as an internal standard. The HR-ESI-MS were done using a Bruker Bioapex-FTMS with electrospray ionization. The chromatographic adsorbents were silica gel G₆₀ (60–120 mesh, Merck, Darmstadt, Germany), C₁₈-RP silica gel (230–400 mesh, Merck, Darmstadt, Germany), MN-polyamide-SC-6 (50–160 μm , Sorbent Technologies, Norcross, GA, USA), SephadexTM LH-20 (Mitsubishi Kagaku, Tokyo, Japan), and Diaion[®] HP-20 (Sorbent Technologies, Norcross, GA, USA). TLC was conducted on pre-coated silica 60F₂₅₄ aluminum sheets, 0.25 mm and RP-18 F₂₅₄, 0.25 mm (E-Merck), Darmstadt, Germany).

3.2. Plant material

The aerial parts of *A. pavonina* were collected in August 2017 from Aswan Botanical Garden, Aswan, Egypt. Dr. Hafeez Rofaeel has authenticated the plant. A voucher specimen (29,313) has been deposited at the herbarium of Flora and Phytotaxonomy Research, Horticultural Research Institute, Agricultural Research Center, Dokki (Cairo), Egypt.

3.3. Extraction and isolation

The dried pulverized aerial parts (4.5 kg) were repeatedly macerated using 70% methanol till exhaustion. A dried residue of 295 g was obtained after the concentration of the combined hydro-alcoholic extracts at 40 °C under reduced pressure. The obtained residue was re-suspended in distilled water and partitioned successively using *n*-

hexane, dichloromethane, and ethyl acetate to give three fractions (F₁–F₃), respectively. The remaining aqueous solution from the partitioning process was dried to provide F₄. Detailed information about the chromatographic separation of each compound is included in the [supplementary material](#).

3.3.1. 5-[1',4'-Dihydroxy-2',6'-dimethyl-6'-carboxy-2'-(2''-methyl succinyloxy) cyclohexyl] -3-methyl-2E, 4E-pentadienoic acid

(1): White powder; $[\alpha]_D^{20} -129.8$ (MeOH, $c = 0.1$); UV λ_{\max} (log ϵ) nm (MeOH); 298 (4.03), ¹H and ¹³C-NMR spectral data (DMSO-*d*₆; 500, 125 MHz) see [Table S1](#); HR-ESI-MS m/z 427.1608 [M – H][–] (calcd 427.1604).

3.3.2. Tamarixetin-3-O- α -L-rhamnopyranosyl-(1→2)- β -D-xylopyranoside (3)

Yellow-brown powder; $[\alpha]_D^{20} -149.7$ (MeOH, $c = 0.1$); UV λ_{\max} (log ϵ) nm (MeOH); 257 (4.01) and 361 (3.94), ¹H and ¹³C-NMR spectral data (DMSO-*d*₆; 400, 100 MHz) see [Table S2](#); HR-ESI-MS m/z 593.1504 [M – H][–] (calcd 593.1506) and 617.1482 [M + Na]⁺ (calcd 617.1482).

3.3.3. 3-O- β -D-glucopyranosyl-23-O- β -D-glucopyranosyl-3 β , 11, 20, 22, 23-pentahydroxy-hopane (8)

White powder; $[\alpha]_D^{20} -78.9$ (MeOH, $c = 0.1$); UV λ_{\max} (log ϵ) nm (MeOH); 206 (3.95), ¹H and ¹³C-NMR spectral data (DMSO-*d*₆; 400, 100 MHz) see [Table S3](#); HR-ESI-MS m/z 861.4810 [M + FA – H][–], calcd for C₄₃H₇₃O₁₇[–], 861.4847

3.3.4. Tamarixetin-3-O-(α -L-rhamnopyranosyl)-(1→2)- β -D-galactopyranoside (11)

Yellow-brown powder; $[\alpha]_D^{20} -48.9$ (MeOH, $c = 0.1$); UV λ_{\max} (log ϵ) nm (MeOH); 255 (3.92) and 357 (3.98), ¹H and ¹³C-NMR spectral data (DMSO-*d*₆; 400, 100 MHz) see [Table S2](#); HR-ESI-MS m/z [M + Na]⁺ at m/z 647.1507 (calcd 647.1588 C₂₈H₃₂O₁₆Na⁺).

3.3.5. Tamarixetin-3-O-(α -L-rhamnopyranosyl-(1→2))- [α -L-rhamnopyranosyl (1→6)]- β -D-galactopyranoside (12)

Yellow-brown powder; $[\alpha]_D^{20} -26.7$ (MeOH, $c = 0.1$); UV λ_{\max} (log ϵ) nm (MeOH); 258 (3.90) and 360 (4.05), ¹H and ¹³C-NMR spectral data (DMSO-*d*₆; 400, 100 MHz) see [Table S2](#); HR-ESI-MS m/z 769.2227 [M – H][–] (calcd 769.2191 C₃₄H₄₁O₂₀[–]) and 805.1998 [M + Cl][–] (calcd 805.2036 C₃₄H₄₃O₂₀Cl[–]).

3.4. Biological evaluations

3.4.1. Chemicals and reagents

Fetal bovine serum (FBS) was purchased from Grand Island, NY, USA). Dimethyl sulfoxide (DMSO), Tumor necrosis factor alpha (TNF- α) ELISA kit, LPS (Escherichia coli, serotype O55:B5) and 3-(4,5-dimethyl-diazol-2-yl)-2,5-diphenyltetrazolium bromide (MTT) were purchased from Sigma–Aldrich (St. Louis, MO, USA). Dulbecco's modified Eagle's medium (DMEM) was purchased from Invitrogen (Life Technologies). TRizol was purchased from Invitrogen (USA). PCR primers for TNF- α and β -actin genes were synthesized and purchased from Vivantis Technologies (Malaysia). 2,2-diphenyl-1-picrylhydrazyl (DPPH) assay kits was purchased from BioVision, Milpitas (USA).

3.4.2. Cell culture, treatments, and measurements of cell viability

In a DMEM solution, BV2 microglial cells were cultured. The cells were then seeded into 24-well plates (cell density 1.2–1.8 10,000 cells/well) and incubated for 24 h at 37 °C. To determine whether the phytochemicals exhibited any cytotoxicity in BV2 cells, the cells were treated with the tested phytochemicals (from 0.4 μM to 100 μM). Control cells were treated with serum-free media containing 1 percent DMSO at the same time. MTT assay was performed after 24 h of treatment, as previously described (van Meerloo et al. 2011).

3.4.3. The anti-inflammatory activities of the tested phytochemicals by measuring mRNA and protein levels of TNF-α in LPS-BV2 microglial cells

In a DMEM solution, BV2 microglial cells were cultured. The cells were then seeded into 24-well plates (cell density; 1.2–1.8, 10,000 cells/well) and incubated for 24 h at 37 °C. Briefly, 1 μg/mL LPS and the tested phytochemicals at the indicated concentrations (from 100 – 0.4 μM) were added in serum-free media for 24 h. Instead, serum-free media containing 1% DMSO was used to treat control cells. The culture media were gently collected and centrifuged for 10 minutes at 1,500 rpm at 4 °C, and the supernatants were collected. The levels of mRNA and protein of TNF-α were determined by qRT-PCR and ELISA kit, respectively.

3.4.4. Determination of mRNA expression of TNF-α by quantitative real-time polymerase chain reaction qRT-PCR

Total RNA was extracted from cell lysates using TRIzol reagent according to the manufacturer's instructions. The RNA was then reversed to create cDNA. For qRT-PCR, SYBR Green PCR Master Mix was used. The relative differences in expression between groups were expressed using Ct values. Data were normalized with β-actin. Relative differences between control and treatment groups were calculated. Primers sequences for TNF-α and β-actin were listed in (Table S7, [supplementary material](#)).

3.4.5. The antioxidant activities of the tested phytochemicals using DPPH antioxidant assay

The antioxidant activities of the tested phytochemicals and trolox were evaluated using the DPPH scavenging assay. Briefly, in a 96-well plate, the DPPH solution was first distributed to each well, and then different concentrations of each tested phytochemical (100–0.1 ng/ml) were added to each well. The plate was incubated for 30 min at room temperature in the dark, and finally, absorbance was recorded at 595 nm wavelength. To authenticate the process, trolox at different concentrations were used as a standard. The degree of scavenging was calculated by the following equation:

$$\text{Scavenging effect (\%)} = \{(\text{Absorbance of control} - \text{Absorbance of sample}) / \text{Absorbance of control}\} \times 100$$

3.4.6. Statistical analysis

All values were analyzed by the GraphPad Prism 7.0 (GraphPad software, USA) and expressed as mean ± SEM. All the statistical analyses were performed using ANOVA

test followed by turkey's post hoc comparison test applied across all groups. Differences with $P < .05$ were considered statistically significant.

4. Conclusions

Five new compounds were reported from *A. pavonina* L. aerial parts. Except for **5**, all tested compounds showed higher antioxidant activities than the control, trolox. Compounds **4**, **5**, **9**, and **11** showed anti-inflammatory potentials as indicated by TNF- α suppression in LPS-stimulated BV2 cells, with **11** having the greatest inhibitory effect on TNF- α protein and m-RNA levels. These findings revealed the antioxidant and anti-inflammatory attributes of *A. pavonina* components, which deserve further investigations.

Acknowledgements

This research was supported financially by Egyptian Government and the National Centre of Natural Products Research (NCNPR), School of Pharmacy, University of Mississippi, USA. Research reported in this publication was also supported by an Institutional Development Award (IDeA) from the National Institute of General Medical Sciences of the National Institutes of Health under award number P20GM130460. We are thankful to Dr. Baharathi Avula for providing HRESIMS.

Disclosure statement

The authors declare no conflict of interest.

Funding

This research was supported financially by Egyptian Government and the National Centre of Natural Products Research (NCNPR), School of Pharmacy, University of Mississippi, USA. Research reported in this publication was also supported by an Institutional Development Award (IDeA) from the National Institute of General Medical Sciences of the National Institutes of Health under award number P20GM130460.

ORCID

Shaymaa M. Mohamed  <http://orcid.org/0000-0001-7768-0890>

Emad H. M. Hassanein  <http://orcid.org/0000-0003-4865-2342>

References

- Adell J, Barbera O, Alberto Marco J. 1988. Flavonoid glycosides from *Anthyllis sericea*. *Phytochemistry*. 27(9):2967–2970.
- Aderogba MA, Kgatle DT, McGaw LJ, Eloff JN. 2012a. Isolation of antioxidant constituents from *Combretum apiculatum* subsp. *apiculatum*. *South African J Bot*. 79:125–131.
- Aderogba MA, Kgatle DT, McGaw LJ, Eloff JN. 2012b. Isolation of antioxidant constituents from *Combretum apiculatum* subsp. *apiculatum*. *South Afr J Bot*. 79:125–131.
- Agrawal PK. 1989. Carbon-13 NMR of flavonoids. Amsterdam; Oxford; New York; Tokyo: Elsevier.

- Ali MS, Ahmed F, Azhar I, Pervez MK. 2005. Pavonin: A new five-membered lactone from *Adenanthera pavonina* Linn. (Mimooaceae). *Nat Prod Res.* 19(1):37–40.
- Choy KW, Murugan D, Leong XF, Abas R, Alias A, Mustafa MR. 2019. Flavonoids as natural anti-inflammatory agents targeting nuclear factor-kappa B (NFκB) signaling in cardiovascular diseases: A mini review. *Front Pharmacol.* 10(OCT):1295.
- Fernando WIT, Attanayake AMKC, Perera HKI, Sivakanesan R, Jayasinghe L, Araya H, Fujimoto Y. 2019. Isolation, identification and characterization of pancreatic lipase inhibitors from *Trigonella foenum-graecum* seeds. *South Afr J Bot.* 121:418–421.
- Gennaro A, Merlini L, Nasini G. 1972. Leguminosae flavonoids from *Adenanthera pavonina*. *Phytochemistry.* 11(4):1515.
- Giollo A, Cioffi G, Ognibeni F, Orsolini G, Dalbeni A, Bixio R, Adami G, Fassio A, Idolazzi L, Gatti D, et al. 2021. Tumour necrosis factor inhibitors reduce aortic stiffness progression in patients with long-standing rheumatoid arthritis. *Arthritis Res Ther.* 23(1):1–9.
- Habib ES, El-Bsoumy E, Ibrahim AK, Helal MA, El-Magd MA, Ahmed SA. 2020. Anti-inflammatory effect of methoxyflavonoids from *Chiliadenus montanus* (*Jasonia Montana*) growing in Egypt. *Nat Prod Res.*: 1–5.
- Halaris A, Meresh E, Fareed J, Hoppensteadt D, Kimmons S, Sinacore J. 2012. 2. Tumor Necrosis Factor alpha as a biomarker in major depressive disorder. *Brain Behav Immun.* 26:51.
- Khare CP. 2007. *Adenanthera pavonina* Linn. In: *Indian Medicinal Plants*. New York: Springer Verlag. p. 18.
- Lindamulage IKS, Soysa P. 2016. Evaluation of anticancer properties of a decoction containing *Adenanthera pavonina* L. and *Thespesia populnea* L. *BMC Complement Altern Med.* 16(1):1–8.
- Ma X, Wu L, Ito Y, Tian W. 2005. Application of preparative high-speed counter-current chromatography for separation of methyl gallate from *Acer truncatum* Bunge. *J Chromatogr A.* 1076(1–2):212–215.
- Medzhitov R. 2010. Inflammation 2010: New adventures of an old flame. *Cell.* 140(6):771–776.
- Mohammed RS, Zeid AHA, El-Kashoury EA, Sleem AA, Waly DA. 2014. A new flavonol glycoside and biological activities of *Adenanthera pavonina* L. leaves. *Nat Prod Res.* 28(5):282–289.
- Nair MP, Mahajan S, Reynolds JL, Aalinkel R, Nair H, Schwartz SA, Kandaswami C. 2006. The flavonoid quercetin inhibits proinflammatory cytokine (tumor necrosis factor alpha) gene expression in normal peripheral blood mononuclear cells via modulation of the NF-kappa beta system. *Clin Vaccine Immunol.* 13(3):319–328.
- Okawa M, Kinjo J, Nohara T, Ono M. 2001. DPPH (1,1-diphenyl-2-picrylhydrazyl) radical scavenging activity of flavonoids obtained from some medicinal plants. *Biol Pharm Bull.* 24(10):1202–1205.
- Olajide OA, Echianu CA, Adedapo ADA, Makeinde JM. 2004. Anti-inflammatory studies on *Adenanthera pavonina* seed extract. *Inflammopharmacology.* 12(2):196–202.
- Owor RO, Bedane KG, Openda YI, Zühlke S, Derese S, Ong'amo G, Ndakala A, Spittler M. 2020. Synergistic anti-inflammatory activities of a new flavone and other flavonoids from *Tephrosia hildebrandtii* vatke. *Nat Prod Res.*35(22): 1–8.
- Peng X, Zheng Z, Cheng KW, Shan F, Ren GX, Chen F, Wang M. 2008. Inhibitory effect of mung bean extract and its constituents vitexin and isovitexin on the formation of advanced glycation endproducts. *Food Chem.* 106(2):475–481.
- Phechmookha T, Sritularak B, Likhitwitayawuid K. 2012. New phenolic compounds from *Dendrobium capillipes* and *Dendrobium secundum*. *J Asian Nat Prod Res.* 14(8):748–754.
- Riaz N, Feroze K, Saleem M, Musaddiq S, Ashraf M, Alam U, Mustafa R, Jabeen B, Ahmad I, Jabbar A. 2013. Oligocephlate, a new α -glucosidase inhibitory neohopane triterpene from *Vernonia oligocephala*. *J Chem Soc Pakistan.* 35(3):972–975.
- Rodríguez-Deleón E, Bah M, Jiménez-Halla JOC, Bonilla-Cruz J, Estévez M, Báez JE. 2019. Synthesis and characterization of segmented poly(ester-urethane)s (PEUs) containing carotenoids. *Polym Chem.* 10(48):6580–6587.
- Sasaki H, Nishimura H, Morota T, Katsuhara T, Chin (Chen Zhengxiong) M, Mitsuhashi H. 1991. Norcarotenoid glycosides of *Rehmannza glutinosa*. *Phytochemistry.* 30(5):1639–1644.

- Shahat AA, Apers S, Van Miert S, Claeys M, Pieters L, Vlietinck A. 2001. Structure elucidation of three new acetylated flavonoid glycosides from *Centaurium spicatum*. *Magn Reson Chem.* 39(10):625–629.
- van Meerloo J, Kaspers GJL, Cloos J. 2011. Cell sensitivity assays: The MTT assay. In: *Methods in Molecular Biology*. Vol. 731. Clifton, NJ: Springer Science + Business Media, LLC. p. 237–245.
- Wang RX, Zhou M, Ma HL, Qiao YB, Li QS. 2021. The role of chronic inflammation in various diseases and anti-inflammatory therapies containing natural products. *ChemMedChem.* 16(10): 1576–1592.
- Wilkins AL, Bremer J, Ralph J, Holland PT, Ronaldson KJ, Jager PM, Bird PW. 1989. A one- and two-dimensional ^{13}C and ^1H N.M.R. study of some triterpenes of the hopane, stictane and flavicene groups. *Aust J Chem.* 42(2):243–257.
- Wongrakpanich S, Wongrakpanich A, Melhado K, Rangaswami J. 2018. A comprehensive review of non-steroidal anti-inflammatory drug use in the elderly. *Aging Dis.* 9(1):143–150.
- Xu WH, Jacob MR, Agarwal AK, Clark AM, Liang ZS, Li XC. 2009. Flavonol glycosides from the native American plant *Gaura longiflora*. *Heterocycles.* 78(10):2541–2548.
- Yasukawa K, Ogawa H, Takido M. 1990. Two flavonol glycosides from *Lysimachia nummularia*. *Phytochemistry.* 29(5):1707–1708.
- Yasukawa K, Sekine H, Takido M. 1989. Two flavonol glycosides from *Lysimachia fortunei*. *Phytochemistry.* 28(8):2215–2216.